16B.6 Climatology of near-storm environments with convective modes for significant severe thunderstorms in the contiguous United States

Richard L. Thompson*, Bryan T. Smith, Jeremy S. Grams, Andrew R. Dean, and Chris Broyles
Storm Prediction Center
Norman, OK

1. Introduction

Proximity soundings have a long history of use in identifying the characteristics of severe storm environments, dating back to the 1940s (Showalter and Fulks 1943) and 1950s (e.g., Fawbush and Miller 1954; Beebe 1955, 1958). This early work has continued into the past two decades when additional proximity sounding samples were constructed by Johns et al. (1993), Rasmussen and Blanchard (1998; hereafter RB98), Rasmussen (2003), and Craven and Brooks (2004; hereafter CB04). These studies either relied on implicit assumptions (e.g., supercells produced all ≥ 2 inch diameter hail in RB98), or large sample sizes but no explicit information regarding storm type (CB04). More recent work by Thompson et al. (2003; hereafter T03), Thompson et al. (2007; hereafter T07), Davies (2004), and Davies and Fischer (2009) used hourly Rapid Update Cycle (RUC) model (Benjamin et al. 2004) analysis profiles to represent the near-storm environment associated with radar-identified supercells and other storm types. These studies provided valuable information regarding storm environment, especially with respect to supercells and tornado production, yet they focused on specific events or storm modes, and the sample sizes were too small to make any definitive statements regarding the frequency of occurrence of different storm modes.

Trapp et al. (2005) developed a relatively large sample of convective modes associated with tornadoes from 1999-2001 across the contiguous United States, using regional radar reflectivity mosaics of relatively coarse spatial and temporal resolution. Somewhat more detailed convective mode categorizations were documented by Gallus et al. (2008) for a 10 state region in the summer, and this was followed by Duda and Gallus (2010) for the same region, with the addition of an estimate of supercell occurrence. These studies cataloged a larger number of convective mode cases than the prior proximity sounding work such as T07 and Davies and Fischer (2009), yet they did not consider environmental information. Thompson et al. (2008) combined a simplified convective mode classification scheme with RUC model and the Storm Prediction Center (SPC) mesoanalysis environmental information to examine near-storm convective parameters in comparison to established severe weather "checklist" variables dating back to the 1950s.

In Part I of this study, Smith et al. (2010, this volume; hereafter S10) documents the development of a large (17037) sample of convective mode cases associated with tornadoes, ≥ 2 inch hail (hereafter sighail), and 65 kt or greater convective wind gusts (hereafter sigwind) across the continental United States. Please refer to S10 for additional details regarding the classification scheme. Building on the work of S10, we have included near-storm environmental information associated with each severe storm and convective mode case. The ultimate goal of this work is to provide a representative sample of severe storm events and associated convective modes and environmental information. Environmental information can be combined with severe storm mode information to improve the diagnoses and short term forecasts of tornadoes and other significant severe thunderstorm events. In the following section we detail our methodology and data collection, and in section 3 we present an analysis of convective modes and environmental information focusing on tornadoes. Section 4 summarizes our findings and outlines continuing and future work related to the SPC convective database.

2. Data and methodology

All tornado, sighail and sigwind reports for the period 2003-2009 were filtered for the largest magnitude report per hour on a 40 x 40 km RUC model analysis grid (Benjamin et al. 2004), and the time filtering assigns each report to the closest prior analysis hour. This filtering procedure produced a sample of 17037 severe thunderstorm

*Corresponding author address: Richard L. Thompson, NOAA/NWS/NCEP/Storm Prediction Center, 120 David L. Boren Blvd., Suite 2300, Norman, OK 73072. Richard.Thompson@noaa.gov

grid-hour events, including 8176 tornadoes, 3361 sighail, and 5500 sigwind events. The hourly RUC analysis grids form the foundation of the SPC hourly mesoanalyses (Bothwell et al. 2002), where hundreds of sounding-derived parameters are calculated at each analysis grid point. The RUC analyses at the lowest model level are used as a first-guess field in an objective analysis of the hourly surface observations, but no further modification of the model profiles is attempted. An archive of a subset of these convective parameters (e.g., Schneider and Dean 2008) is maintained at the SPC, and these data provide the basis for the analyses herein.

The basic convective modes identified were supercells (both right-moving (RM) and left-moving (LM) supercells), quasi-linear convective systems (QLCS), and disorganized cells or clusters. Two additional subsets included storms with marginal supercell characteristics (after T03), and a linear hybrid mode with mixed characteristics of both RM in a line and QLCS (see S10 for a more detailed discussion regarding the practical difficulties of convective mode categorization). The derived parameters from the SPC mesoanalysis system were determined for each severe weather report and convective mode, forming the equivalent of a large close proximity sounding relational database for known storm types and severe weather events.

a. Data accuracy and representativeness

As with any attempt at assigning single point variables to represent a storm environment, concerns regarding the accuracy and representativeness of the data must be considered. Brooks et al. (1994) discussed many of the concerns with arriving at "proximity" for a storm environment, while Potvin et al. (2010) considered the impacts of varying proximity criteria. Compared to rawinsonde observations, the SPC mesoanalysis system has the advantage of producing hourly environmental information on a 40 x 40 km grid, which provides much greater spatial and temporal resolution than the observed sounding network. The background RUC analyses incorporate a wide range of synoptic (e.g., standard 00/12 UTC rawinsonde observations) and asynoptic data (e.g., surface mesonet data, aircraft observations, etc.) to provide a reasonably accurate depiction of the synoptic and mesoscale environment. The most consistent biases noted by T03 in the RUC profiles were near the ground, where the SPC mesoanalysis system performs an objective analysis of the actual surface observations using the RUC analysis as a first guess field. The result is an hourly surface analysis that attempts to remove RUC biases at the surface.

The SPC mesoanalysis approach does not correct for all potential errors. Given the propensity for severe thunderstorms to occur in the vicinity of baroclinic zones with strong horizontal gradients of temperature, moisture, and wind, small phase errors can result in somewhat misleading information for a particular storm case (i.e., a tornado occurs at 00:45 after an hour, but a warm front does not reach the same grid point until shortly after the top of the next hour). In other cases, the background RUC analyses aloft may be questionable. The Greensburg, KS EF5 tornado case provides a specific example of this type of problem. The nearest RUC grid point profiles were apparently too dry just above the surface, and this strongly impacted parameters such as the lowest 100 mb mean-layer CAPE (MLCAPE) compared to the surface-based (SB) parcel counterpart (e.g., MLCAPE of 883 J kg^{-1} versus SBCAPE of 3487 J kg^{-1}). Though we have made no attempt to correct any individual errors, the operational experience of the authors and the prior work by T03 suggests that a large sample size should minimize the impact of outliers within the sample.

3. Results and discussion

All of the tornado cases were sorted initially by convective mode in order to provide an overview of environmental conditions related to each convective mode type. While a full spectrum of convective modes was documented, a majority of the Schneider and Dean (2008) data are related primarily to supercells and tornadoes. Thus, our main focus concerns tornado and significant tornado (e.g., ≥ F2 damage; hereafter sigtor) production with RM, and a comparison of the supercell-related parameters to other convective mode environments.

We employed an ingredients-based approach (Johns and Doswell 1992) in our evaluation of the storm environments, but it is important to understand the limitations of convective parameters and indices (Doswell and Schultz 2006) since they comprise the majority of our database. The individual parameters can be grouped into measures of vertical wind shear, such as 0-1 km storm-relative helicity (SRH, Davies-Jones et al. 1990; using the storm motion

estimate described by Bunkers et al. 2000) and 0-6 km bulk wind difference (e.g., RB98 and T03 among others), as well as thermodynamic parameters such as MLCAPE using the virtual temperature correction described in Doswell and Rasmussen (1994), and lifting condensation level (MLLCL). Combinations of the aforementioned parameters have been shown to discriminate most strongly between significantly tornadic (F2+ damage) and nontornadic supercells (e.g., Supercell Composite Parameter (SCP) and Significant Tornado Parameter (STP) from T03 and Thompson et al. 2004), while two of the individual shear parameters have been modified to more accurately apply to a wide range of storm environments (i.e., effective SRH (ESRH) and the effective bulk wind difference (EBWD) from T07).

Severe thunderstorms cases that produced less than 2 inch diameter hail or wind gusts less than 65 kt were not part of this database, nor were non-severe thunderstorms due to an unmanageably large number of such cases for manual convective mode classification. The exclusion of these weaker events does not allow a complete assessment of null cases for each event type. Instead, comparison null samples were identified by applying standard proximity sounding criteria (e.g., +/- 3 hours and within 185 km per CB04) to each event type, leaving a subset of sighail and sigwind events with no nearby tornadoes.

a. Tornado environments by convective mode and F-scale damage rating

Tornadoes of all damage class ratings comprised 8176 of the 17037 convective mode cases for our seven year sample across the continental United States (see Table 1 from S10 for detailed information regarding the distribution of specific convective modes). Over the entire sample of tornado events, most-unstable parcel CAPE (MUCAPE) spanned a rather wide range from less than 500 J kg^{-1} on the low end (e.g., 10^{th} percentile bottom "whiskers" in Fig. 1), to in excess of 3000 J kg^{-1}. The tornadic linear convective modes were associated with somewhat lesser MUCAPE compared to discrete and cluster RM, but with substantial overlap between mode types within the parameter space. Environmental influences on storm mode become more apparent when considering EBWD and ESRH (Figs. 2 and 3, respectively). The so-called "organized" severe storm modes such as RM and hybrid linear systems resided within the parameter space associated with supercells in previous studies (e.g., EBWD > 30-40 kt per Fig. 3 and T07), while a gradual transition to weaker vertical shear occurs from the QLCS to marginal RM and disorganized storms. Combining the ingredients into the SCP reveals a similar decrease in values from the RM down to QLCS and disorganized storms (Fig. 4).

The tornado event sample was also sorted to identify variations in storm environments with specific convective modes across tornado damage ratings. As seen in Fig. 5, MLCAPE tended to be a little larger with discrete RM compared to QLCS, though no meaningful differences were noted across the F-scale damage ratings within either mode type. Interestingly, considerably more than 25% of the QLCS events were associated with MLCAPE < 500 J kg^{-1}. The opposite trends were noted with MLLCL heights (Fig. 6), with smaller ranges and moister environments for the significant tornadoes with both RM and QLCS, and drier environments and wider ranges of values for the nontornadic storms. Further analysis indicated that the largest LCL heights accompanied the discrete RM that produced only sighail (RMd nontor in Fig. 6), though these storms were largely confined to the Great Plains.

Measures of deep-layer vertical shear discriminate well between discrete RM and nonsupercell storms (e.g., Weisman and Klemp 1982, RB98, and T03, among others), but not particularly well between the nontor and F0 QLCS and discrete RM (Fig. 7). Differences between the discrete sigtor RM and nontor RM/QLCS are more pronounced when considering the both the 0-6 km bulk wind difference and EBWD, which accounts for the depth of buoyancy. The 0-6 km bulk wind difference shows the least overlap between the sigtor QLCS and nontor QLCS (compared to EBWD). The non-tornadic QLCS events begin to transition downward from the supercell portion of the parameter space for the lower half of the distribution.

Measures of low-level vertical wind shear show greater discrimination, compared to EBWD and 0-6 km bulk wind difference, between the tornado damage rating classes for both QLCS and RM. The 0-1 km bulk wind differences between the nontor discrete RM and the sigtor discrete RM (Fig. 8) were quite pronounced, with a large majority of sigtor (nontor) cases greater (less) than 20 kt, in general agreement with past studies (e.g., Rasmussen 2003 and CB04). Still, the 0-1 km bulk wind difference does not allow effective

differentiation between QLCS and RM for the tornadic storms. The same limitation applies to both 0-1 km SRH and ESRH (not shown).

b. Variations in F-scale damage by environment, storm mode, and mesocyclone strength

Both the sigtor QLCS and sigtor discrete RM occur in the strongest vertical shear environments per Figs. 7 and 8, while weaker instability characterizes the QLCS events (Fig. 5). Differences in storm environments for the tornadic QLCS and discrete RM become more apparent via the nonlinear combination of ingredients in the STP (Fig. 9). The discrete sigtor RM reside in the most volatile combinations of buoyancy and vertical shear, much higher in the parameter space than either of the nontornadic storm samples, and noticeably greater than the tornadic QLCS and weakly tornadic (F0 damage) RM distributions.

The STP was designed to identify the most dangerous supercell tornado environments, yet relatively small sample sizes in prior studies (e.g., T03) precluded examination of STP as a function of F-scale damage with supercells. In Fig. 10, a monotonic increase in STP is noted with increasing F-scale damage ratings for all damage classes and at all percentile ranks, where larger values of STP correspond to more intense tornado damage on average. The relative frequency of tornadoes increases in each F-scale damage category with increasing STP (Table 1), with much higher relative frequencies of larger STP values for the more intense tornadoes. Still, weaker tornadoes dominate the overall frequency distribution across all values of STP since the weakest tornadoes (3186 F0) far outnumber the most intense tornadoes (39 F4-F5). The substantial overlap in the distributions and the tendency for weak tornadoes to far exceed the number of intense tornadoes suggests that confident delineation in damage categories will prove difficult for individual storms during a particular hour, based on storm mode and environment alone. Semi-objective estimates of mesocyclone strength were determined for all of the supercells (cyclonic for the RM and anticyclone for the LM), following the mesocyclone nomograms developed by the Warning ecision Training Branch of the National Weather Service (after Andra 1997 and Stumpf et al. 1998). The mesocyclone strengths appear to be related to the storm environment, as represented by the SCP for the three rotational strength categories shown in Fig. 11. The stronger mesocyclones occurred more commonly in the environments more favorable for RM (i.e., larger SCP). The STP compared to F-scale for RM (Fig. 12) reveals the combined tendency for the more intense (F3+) tornadoes to occur with moderate and strong mesocyclones in environments of relatively large STP, while the RM with weak mesocyclones occur in somewhat marginal environments and do not produce F3+ tornadoes.

Although a composite parameter's primary value is in identifying a co-location of important supercell tornado ingredients, the individual components in the STP should always be examined independently to ascertain the relative contributions of each component.. The instability and vertical shear parameters examined herein do show some ability to discriminate between the sigtor RM and QLCS events, however, accurate forecasts of convective mode are still necessary since the large majority of F3+ tornadoes (83%) occur with discrete or cluster RM. Dial et al. (2010) found that the strength of the low-level forcing for ascent and the orientation of deep-layer shear vectors relative to initiating synoptic boundaries hold promise in delineating between linear and discrete convective modes, in environments otherwise supportive of supercells.

c. Seasonal variations in RM sigtor environments

Seasonal variations in sigtor RM distribution are highlighted in Fig. 13, with clustering of sigtors across the Lower Mississippi and Tennessee Valleys in the winter (DEC-FEB), the central Plains to the Middle Mississippi Valley in the spring (MAR-MAY), the northern Plains in the summer (JUN-AUG), and the Lower Ohio and Mississippi Valleys in the fall (SEP-NOV). The supercell tornado ingredients also show some seasonal and regional variability. Winter and fall MLCAPE values were substantially lower than spring and summer values (Fig. 14), while MLLCL heights (Fig. 15) were similar in distribution to MLCAPE by season. Not surprisingly, vertical wind shear was strongest during the winter (Figs. 16 and 17) where events were clustered across the Lower Mississippi Valley, compared to weaker vertical shear in the summer across the central and northern Great Plains where RM sigtor are clustered. Interestingly, combining the ingredients into the STP (Fig. 18) highlights the more volatile spring environments across the southern and central Plains, where sigtor RM were most common. The spring environments do not display

the largest MLCAPE, lowest MLLCL heights or strongest vertical shear compared to the other seasons, but the spring has no consistent weakness in any of the basic ingredients, such as the relatively smaller MLCAPE in the winter or relatively weaker 0-1 km SRH in the summer.

4. Summary and conclusions

The relational database of severe storm events and environmental parameters maintained at the SPC (Schneider and Dean 2008) has been augmented to include convective mode information for the majority of tornado and significant severe thunderstorm events from 2003-2009. The convective mode assignments were based on manual inspection of level II or level III WSR-88D imagery associated with the radar site closest to each event (S10). This resulted in the identification of 8176 tornado events, 5500 sigwind events, and 3361 sighail events across the continental United States with associated convective mode and environmental information. The convective modes and environments associated with the tornado events were the focus of this preliminary work.

Right-moving supercells dominated tornado production within our sample, thus forming the core of the investigation. The SCP, as well as its constituent components ESRH and EBWD, discriminates well between the disorganized tornadic storms and the three classes of supercells (discrete, cell in cluster, and cell in line), in agreement with the prior work of T03 and T07. The linear hybrid and QLCS cases populated a part of the EBWD and ESRH parameter spaces similar to the supercells, with lesser vertical shear in the "marginal" supercell cases. The discrete and cluster RM occurred in environments of slightly greater MUCAPE, with the linear convective modes displaying MUCAPE approximately 500 J kg^{-1} lower across the distribution. Overall, environmental differences between the supercells and linear modes were relatively small, indicating that environmental information alone is not able to clearly discriminate between storm modes in a practical sense.

Storm attributes such as mesocyclone strength and tornado damage ratings both tended to increase in conjunction with composite parameters supporting supercells and tornadoes (e.g., SCP and STP). Our findings reinforce a diagnostic "recipe" that combines storm environment (e.g., large values of STP) and convective mode (RM) mode with mesocyclone strength to favor the production of the most intense (F3-F5) tornadoes. Specifically, the more common scenario favoring the production of F3+ tornadoes includes multiple and/or long-lived supercells with strong mesocyclones, in an environment characterized by the upper-end of the STP distribution (i.e., >= 4 or so).

Future work includes continued expansion of the database on a yearly basis, with the goal of providing a solid foundation for multi-faceted forecast verification at the SPC. Also, the environmental data archive will be expanded to include a wide range of variables and parameters related to all severe convective events, and not limited to tornadic right-moving supercells emphasized in this initial work.

Acknowledgements: The authors thank Russ Schneider and Steve Weiss of the SPC for their insight and encouragement in the design and development of the convective mode database.

References

Andra, D. L., 1997: The origin and evolution of the WSR-88D mesocyclone recognition nomogram. Preprints, *28th Conf. on Radar Meteor.,* Austin, TX, Amer. Meteor. Soc., 364–365.

Beebe, R. G., 1955: Types of airmasses in which tornadoes occur. *Bull. Amer. Meteor. Soc.*, 36, 349–350.

_____, 1958: Tornado proximity soundings. *Bull. Amer. Meteor. Soc.*, **39**, 195–201.

Benjamin, S. G., and Coauthors, 2004: An hourly assimilation-forecast cycle: The RUC. *Mon. Wea. Rev.*, **32**, 495-518.

Bothwell, P. D., J. A. Hart, and R. L. Thompson, 2002: An integrated three-dimensional objective analysis scheme in use at the Storm Prediction Center. Preprints, *21st Conf. on Severe Local Storms,* San Antonio, TX, Amer. Meteor. Soc., J117–J120.

Brooks, H. E., C. A. Doswell III, and J. Cooper, 1994: On the environments of tornadic and nontornadic mesocyclones. *Wea. Forecasting*, **9**, 606–618.

Bunkers, M. J., B. A. Klimowski, J. W. Zeitler, R. L. Thompson, and M. L. Weisman, 2000:

Predicting supercell motion using a new hodograph technique. *Wea. Forecasting*, **15**, 61–79.

Craven, J. P., and H. E. Brooks, 2004: Baseline climatology of sounding derived parameters associated with deep moist convection. *Nat. Wea. Digest*, **28**, 13-24.

Davies, J. M., 2004: Estimations of CIN and LFC associated with tornadic and nontornadic supercells. *Wea. Forecasting*, **19**, 714-726.

_____, and A. Fischer, 2009: Environmental characteristics associated with nighttime tornadoes. *NWA Electronic Journal of Operational Meteorology*, 2009-EJ3.

Davies-Jones, R. P., D. W. Burgess, and M. Foster, 1990: Test of helicity as a tornado forecast parameter. Preprints, *16th Conf. on Severe Local Storms*, Kananaskis Park, AB, Canada, Amer. Meteor. Soc., 588-592.

Dial, G. L, J. P. Racy, and R. L. Thompson, 2010: Short-term convective mode evolution along synoptic boundaries. Accepted to *Wea. Forecasting.*

Doswell, C. A., III, and E. N. Rasmussen, 1994: The effect of neglecting the virtual temperature correction on CAPE calculations. *Wea. Forecasting*, **9**, 625-629.

_____, and D. M. Schultz, 2006: On the use of indices and parameters in forecasting severe storms. *Electronic J. Severe Storms Meteor*., **1** (3), 1-22.

Duda, J. D., and W. A. Gallus, Jr., 2010: Spring and summer Midwestern severe weather reports in supercells compared to other morphologies. *Wea. Forecasting*, **25**, 190-206.

Fawbush, E. J., and R. C. Miller, 1954: The types of air masses in which North American tornadoes form. *Bull. Amer. Meteor. Soc*., **35**, 154–165.

Gallus, W. A., Jr., N. A. Snook, and E. V. Johnson, 2008: Spring and summer severe weather reports over the Midwest as a function of convective mode: A preliminary study. *Wea. Forecasting*, **23**, 101–113.

Johns, R. H., J. M. Davies, and P. W. Leftwich, 1993: Some wind and instability parameters associated with strong and violent tornadoes. 2. Variations in the combinations of wind and instability parameters. *The Tornado: Its Structure, Dynamics, Prediction, and Hazards*, Geophys. Monogr., No. 79, Amer. Geophys. Union, 583–590.

Potvin, C. K., K. L. Elmore, and S. J. Weiss, 2010: Assessing the impacts of proximity sounding criteria on the climatology of significant tornado environments. *Wea. Forecasting*, **25**, 921-930.

Rasmussen, E. N., and D. O. Blanchard, 1998: A baseline climatology of sounding-derived supercell and tornado forecast parameters. *Wea. Forecasting*, **13**, 1148–1164.

_____, 2003: Refined supercell and tornado forecast parameters. *Wea. Forecasting*, **18**, 530-535.

Schneider, R. S., and A. R. Dean, 2008: A comprehensive 5-year severe storm environment climatology for the continental United States. Preprints, *24th Conf. Severe Local Storms*, Savannah GA., Amer. Meteor. Soc.

Showalter, A. K., and J. R. Fulks, 1943: Preliminary report on tornadoes. U.S. Weather Bureau, 162 pp.

Silverman, B.W., 1986. Density estimation for statistics and data analysis. New York: Chapman and Hall.

Smith, B. T., R. L. Thompson, J. S. Grams, and J. C. Broyles, 2010: Convective modes associated with significant severe thunderstorms in the contiguous United States. Preprints, *25th Conf. on Severe Local Storms*, Denver, Co., Amer. Meteor. Soc.

Stumpf, G. J., A. Witt, E. D. Mitchell, P. L. Spencer, J. T. Johnson, M. D. Eilts, K. W. Thomas, and D. W. Burgess, 1998: The National Severe Storms Laboratory mesocyclone detection algorithm for the WSR-88D. *Wea. Forecasting*, **13**, 304–326.

Thompson, R. L., R. Edwards, J. A. Hart, K. L. Elmore, and P. M. Markowski, 2003: Close proximity soundings within supercell environments obtained from the Rapid Update Cycle., *Wea. Forecasting*, **18**, 1243–1261.

_____, C. M. Mead, and R. Edwards, 2007: Effective storm-relative helicity and bulk shear in supercell thunderstorm environments. *Wea. Forecasting*, **22**, 102-115.

_____, J. S. Grams, and J. Prentice, 2008: Synoptic environments and convective modes associated with significant tornadoes in the continental United States. *Preprints, 24th Conf. on Severe Local Storms*, Savannah, GA., Amer. Meteor. Soc.

Trapp, R. J., S. A. Tessendorf, E. S. Godfrey, and H. E. Brooks, 2005: Tornadoes from squall lines and bow echoes: Part I: Climatological distribution. *Wea. Forecasting*, **20**, 23-33.

Weisman, M. L., and J. B. Klemp, 1982: The dependence of numerically simulated convective storms on wind shear and buoyancy. *Mon. Wea. Rev.*, **110**, 504–520.

Table 1. Cumulative frequency of STP (columns) by tornado F-scale damage (rows). Cumulative frequencies are color-coded gray (0-24%), black (25-49%), bold black (50-74%), and bold red (≥ 75%).

	<0.5	**≥ 0.5**	**≥ 1.0**	**≥ 2.0**	**≥ 4.0**	**≥ 6.0**	**Total #**
None	0.64	0.36	0.21	0.08	0.02	0.01	1888
F0	0.37	**0.63**	0.47	0.26	0.10	0.04	3186
F1	0.28	**0.72**	**0.54**	0.32	0.13	0.04	1745
F2	0.13	**0.87**	**0.70**	0.46	0.22	0.06	663
F3	0.08	**0.92**	**0.83**	**0.58**	0.33	0.11	214
F4+	0.08	**0.92**	**0.92**	**0.77**	0.49	0.31	39

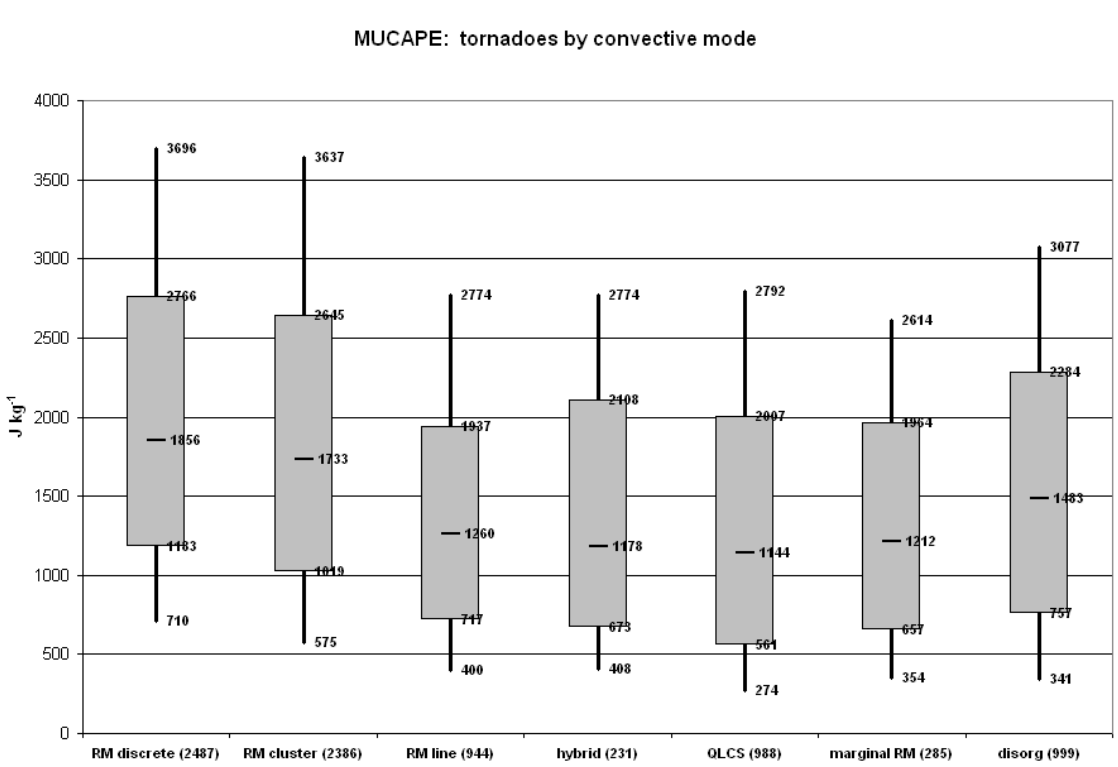

Figure 1. Box and whiskers plot of most-unstable parcel CAPE (J kg^{-1}) for the tornadoes and associated convective modes, where cases with hybrid characteristics of both RM in line and QLCS are denoted as "hybrid", and discrete cells/clusters with no organized structures are denoted as "disorg". The shaded boxes span the 25th to the 75th percentiles, and the whiskers extend upward to the 90th and downward to the 10th percentiles. Median values are marked within the box, and sample sizes for each storm mode are shown in parentheses.

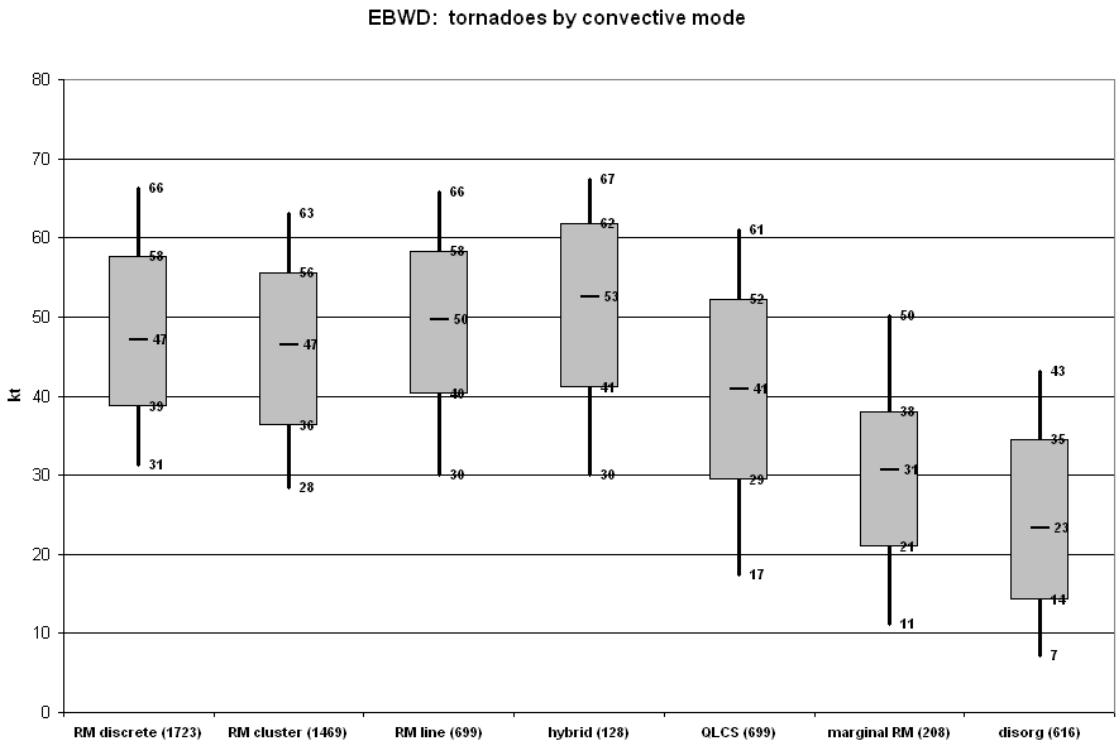

Figure 2. Same as Fig. 1, except for the EBWD (kt).

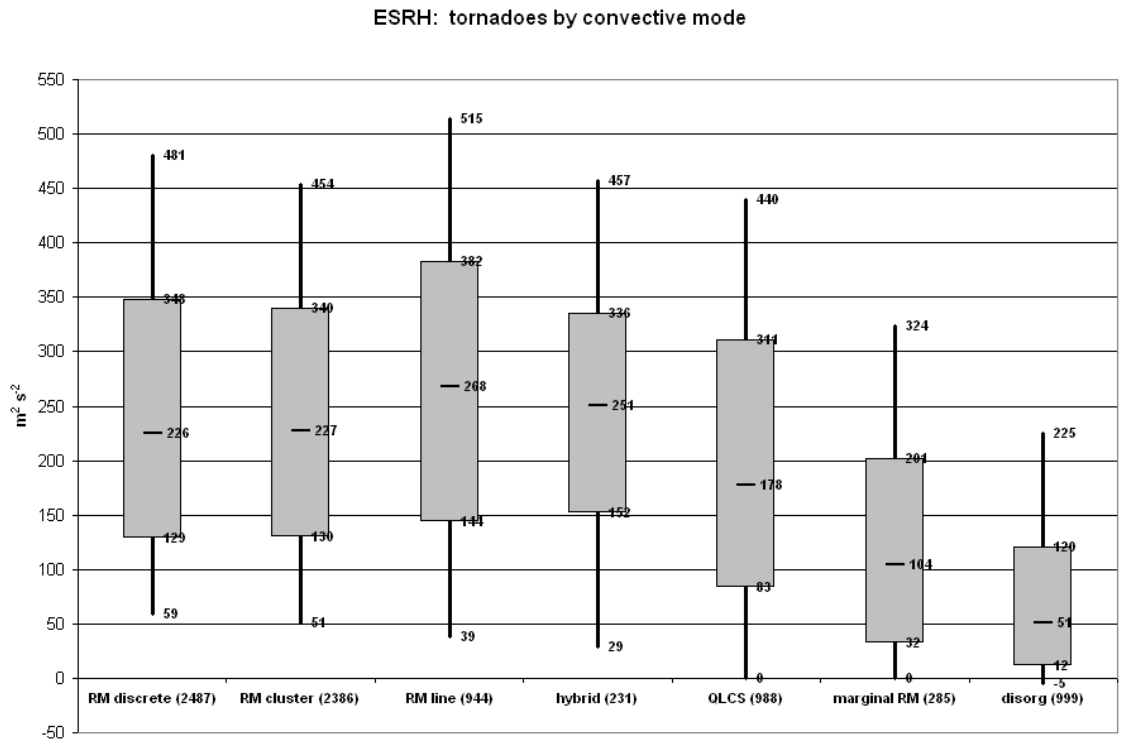

Figure 3. Same as Fig. 1, except for ESRH ($m^2 s^{-2}$).

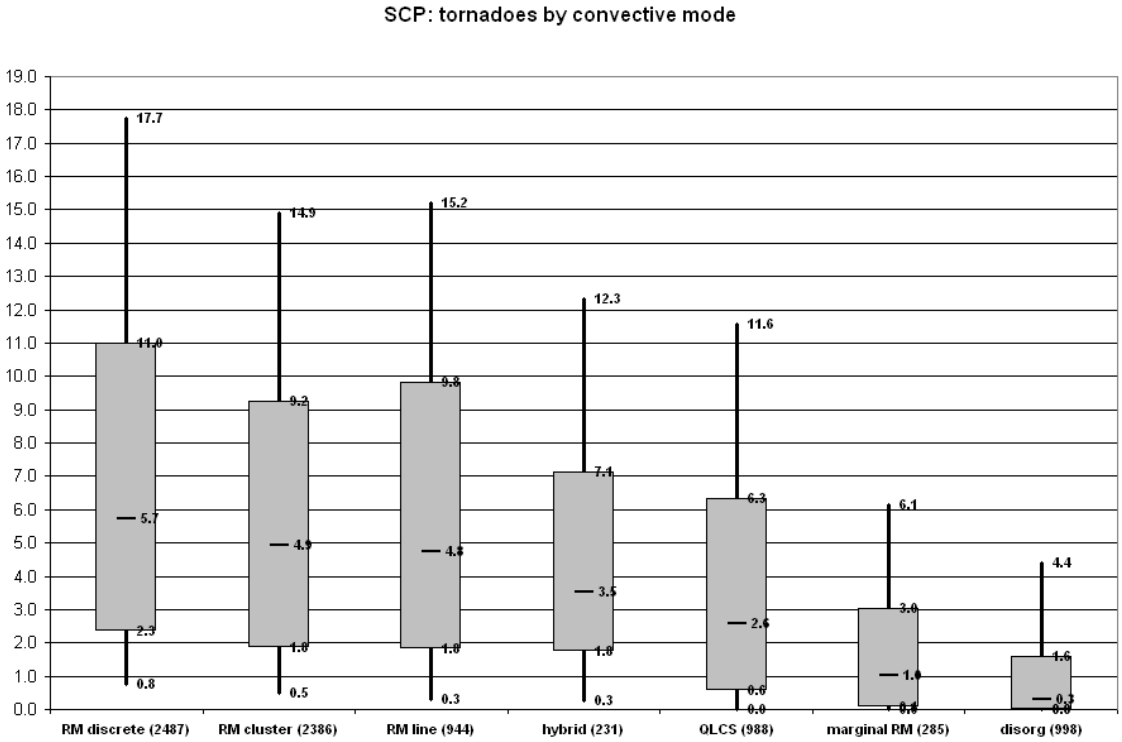

Figure 4. Same as Fig. 1, except for SCP.

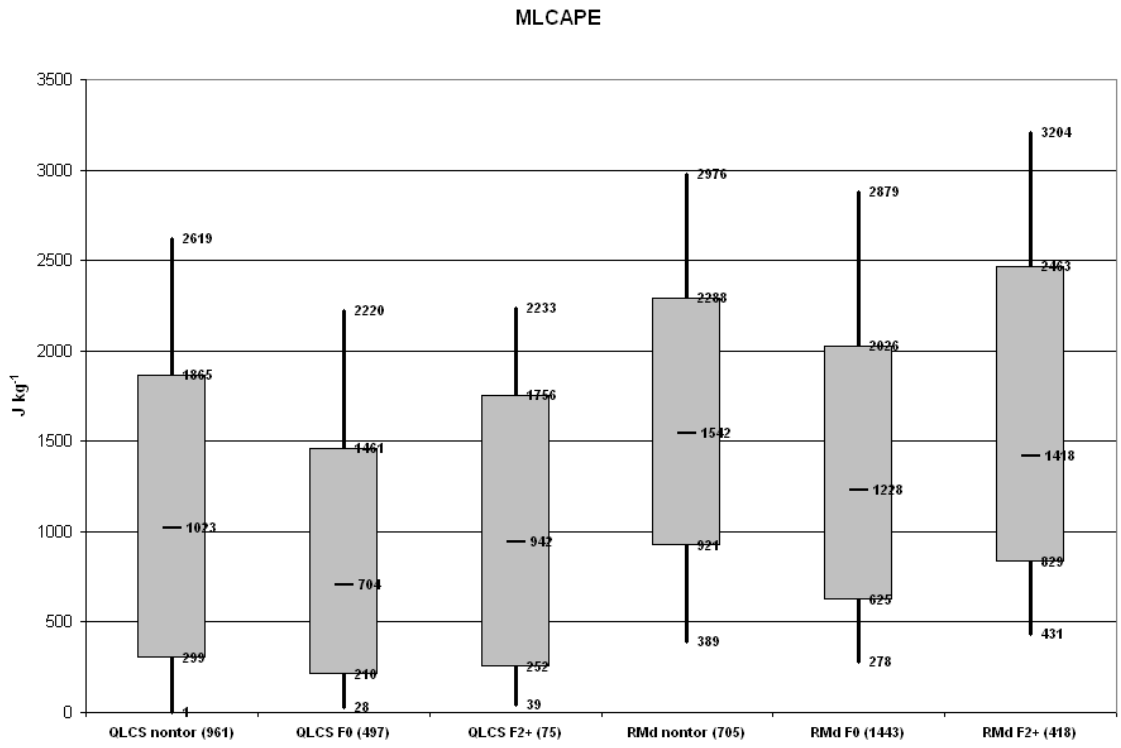

Figure 5. Box and whiskers plot of MLCAPE (J kg^{-1}) for nontornadic (nontor), weak tornado (F0), and significant tornado (F2+) events associated with QLCS and discrete RM (RMd). Other conventions are the same as Fig. 1.

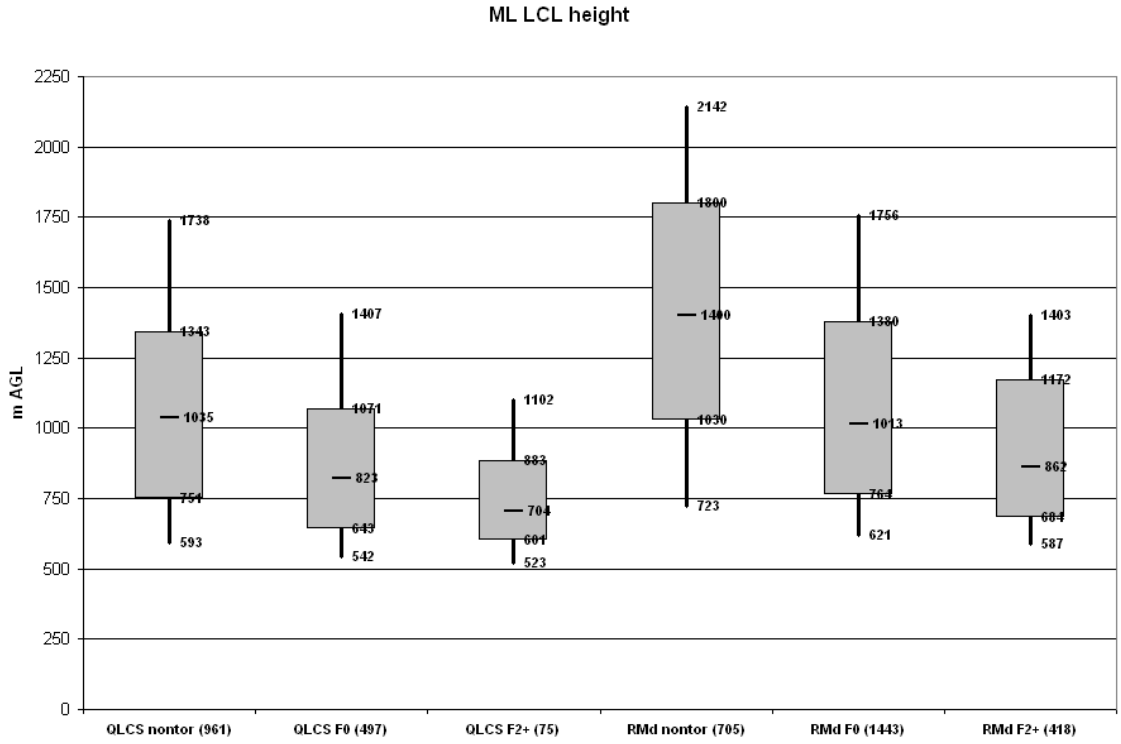

Figure 6. Same as Fig. 5, except for MLLCL height (m AGL).

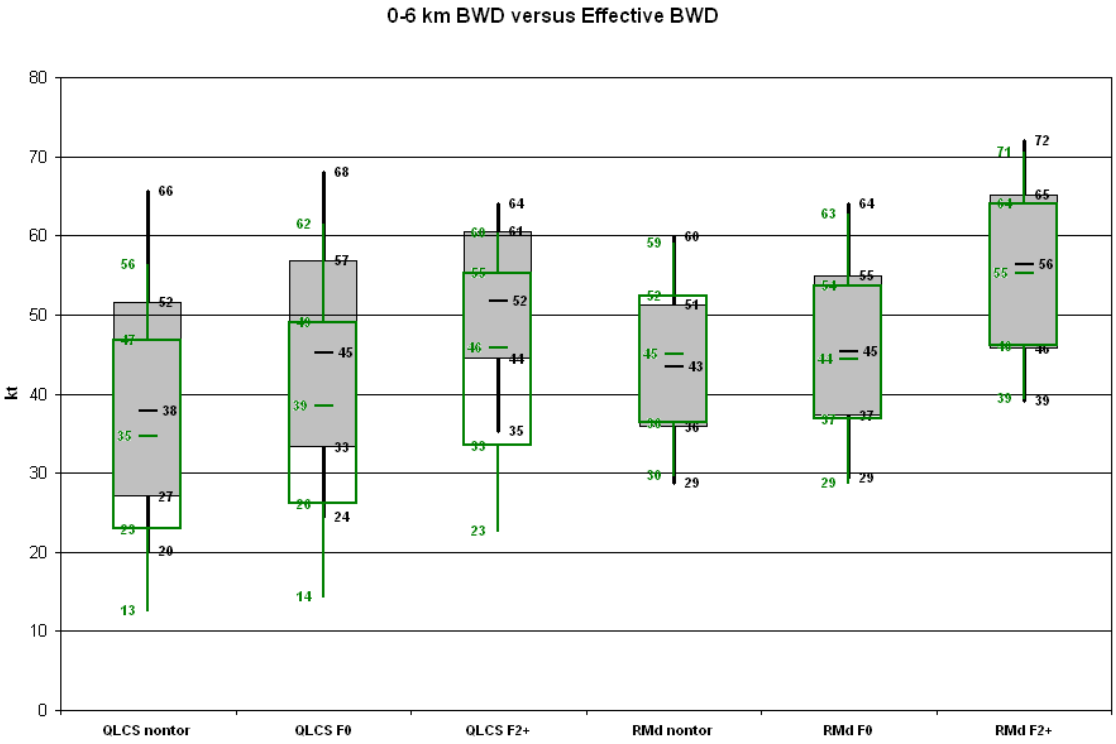

Figure 7. Same as Fig. 5, except for 0-6 km bulk wind difference (kt, solid boxes and black labels on the right) and EBWD (kt, green overlays and green labels on the left).

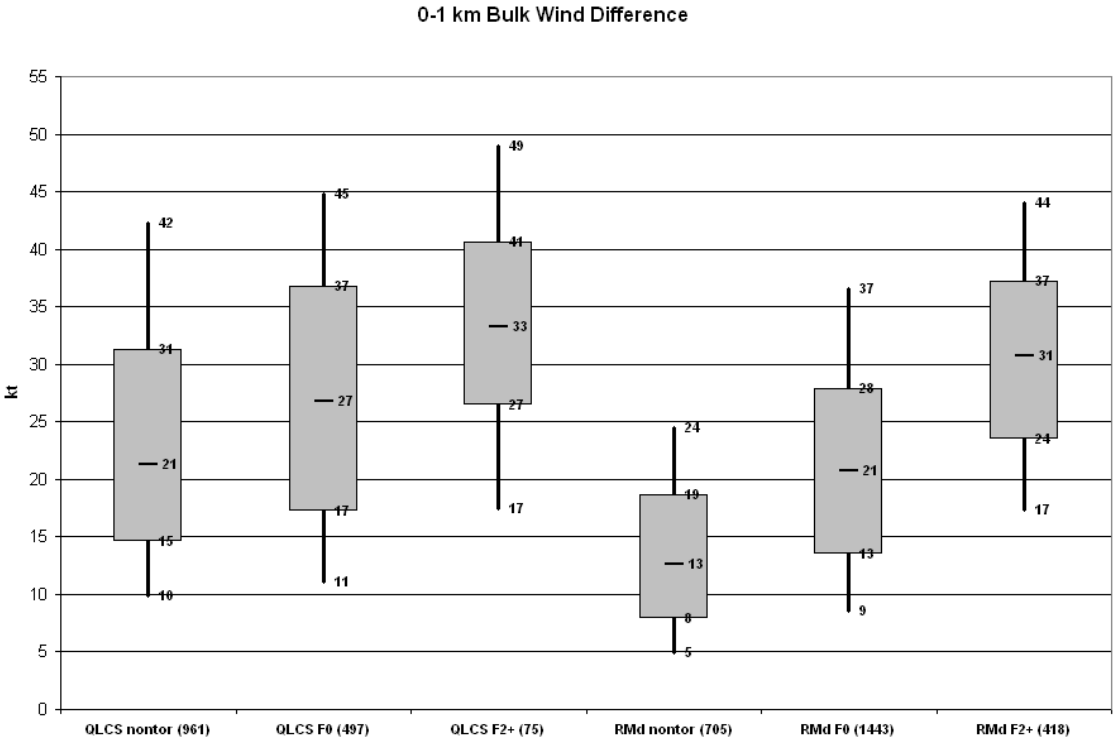

Figure 8. Same as Fig. 5, except for 0-1 km bulk wind difference (kt).

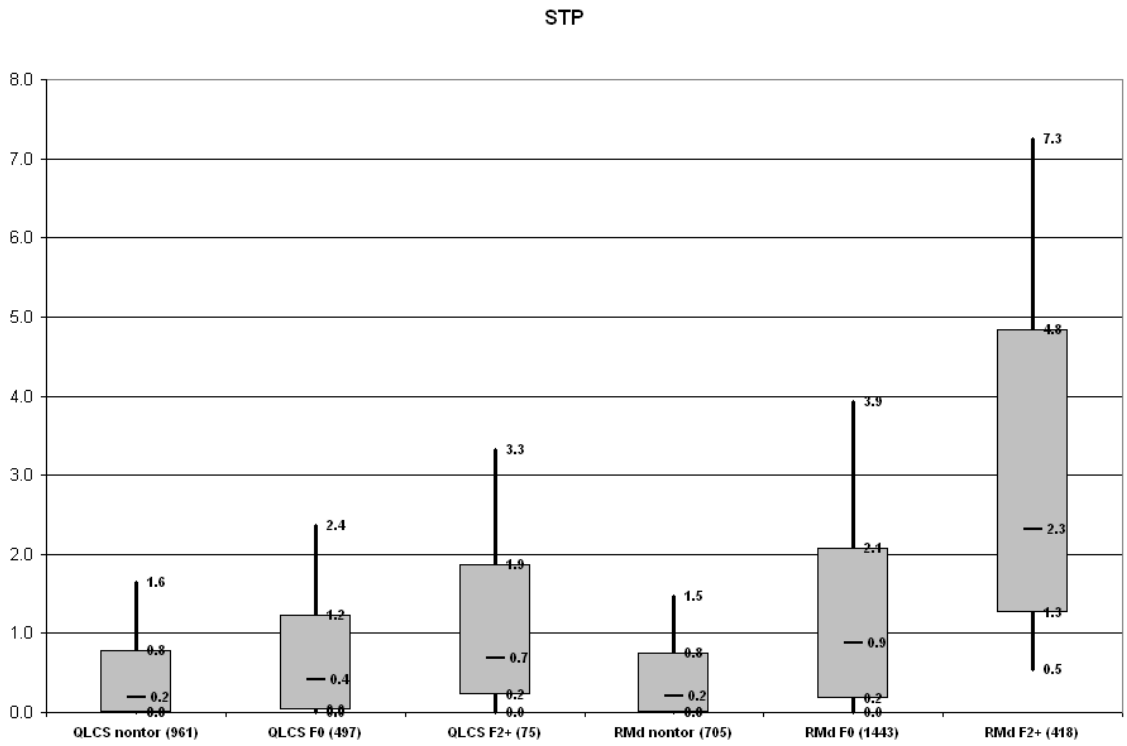

Figure 9. Same as Fig. 5, except for STP.

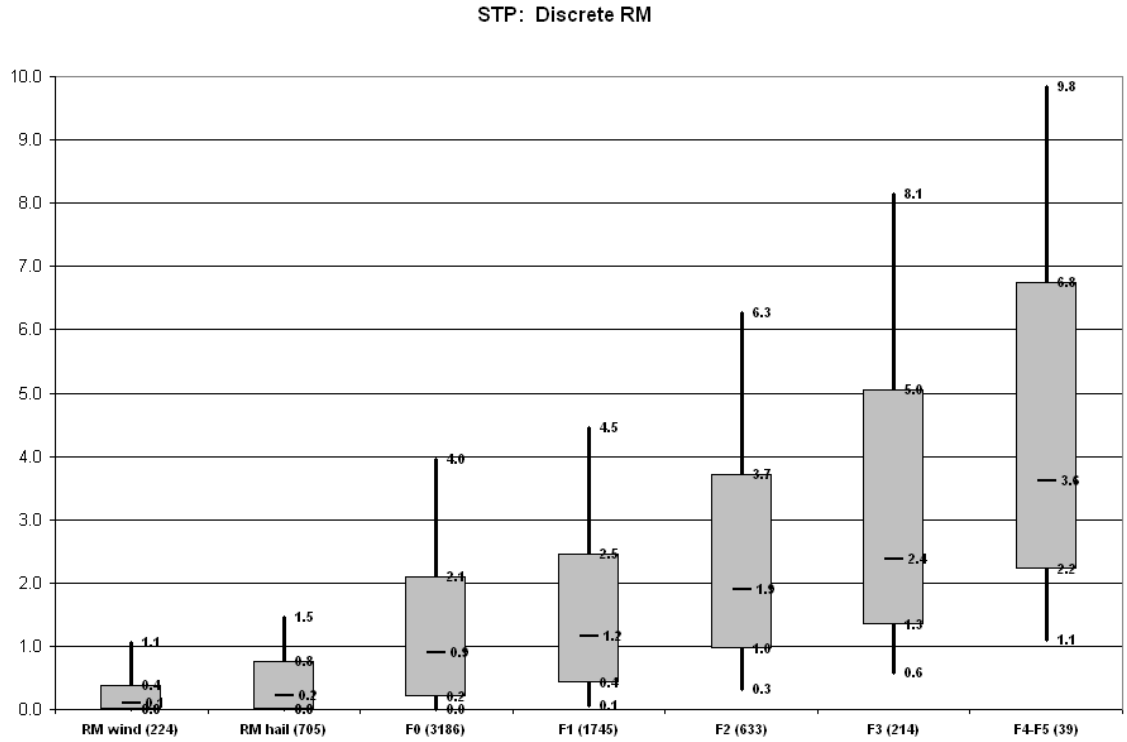

Figure 10. Box and whiskers plot of STP for discrete RM by F-scale damage rating classes, including nontornadic RM that produced sigwind (wind) and sighail (hail). Other conventions are the same as Fig. 1.

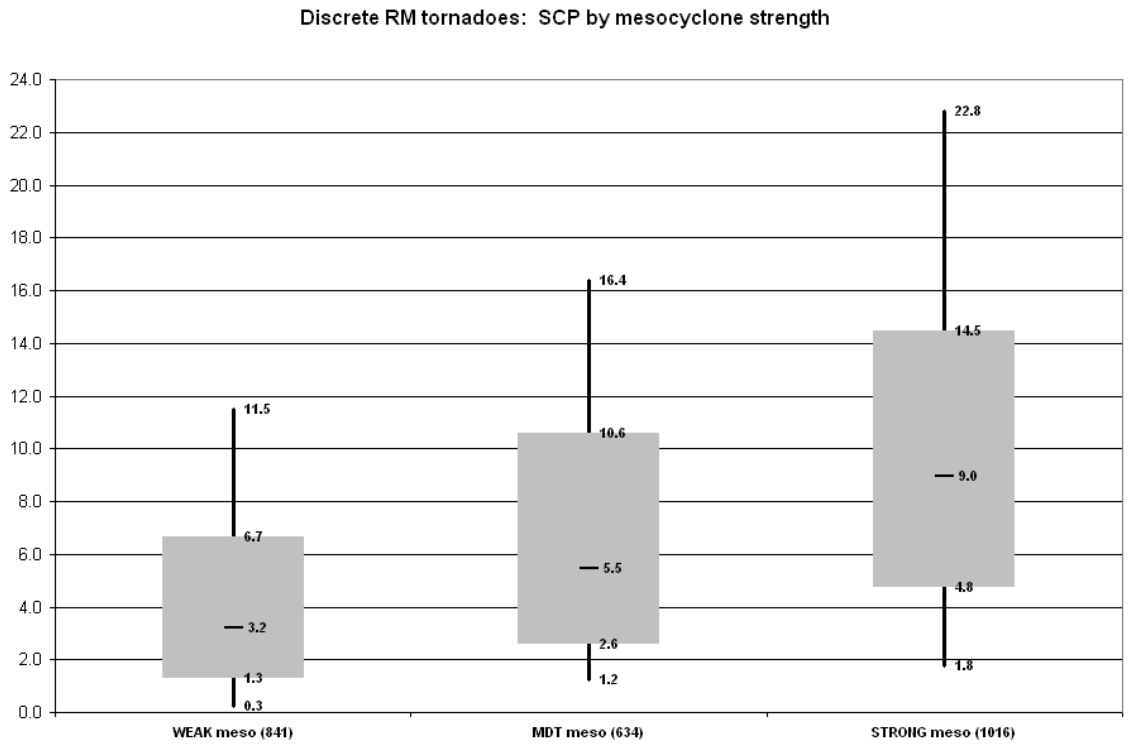

Figure 11. SCP with all tornadic RM for weak, moderate (MDT), and strong mesocylones. Box and whisker conventions are the same as Fig. 1.

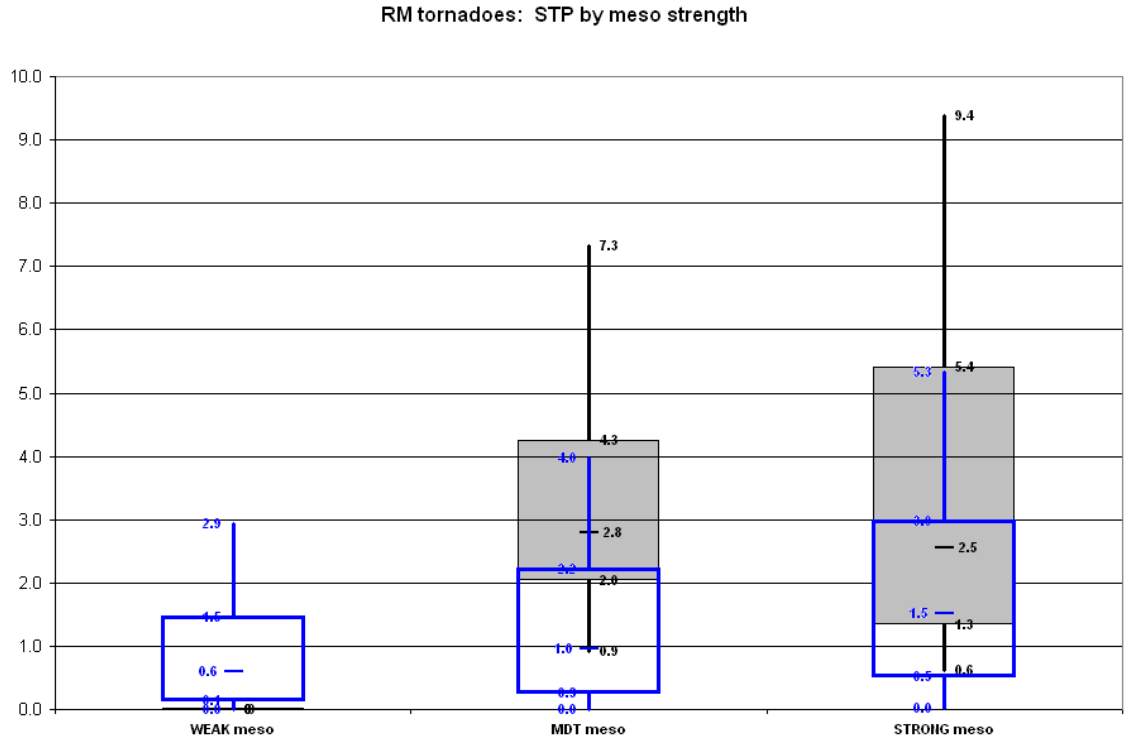

Figure 12. Same as Fig. 11, except for STP. The solid boxes (black labels on the right) denote RM with F3+ tornado damage, and the blue overlays (with labels on the left) represent the RM that produced F0 tornado damage.

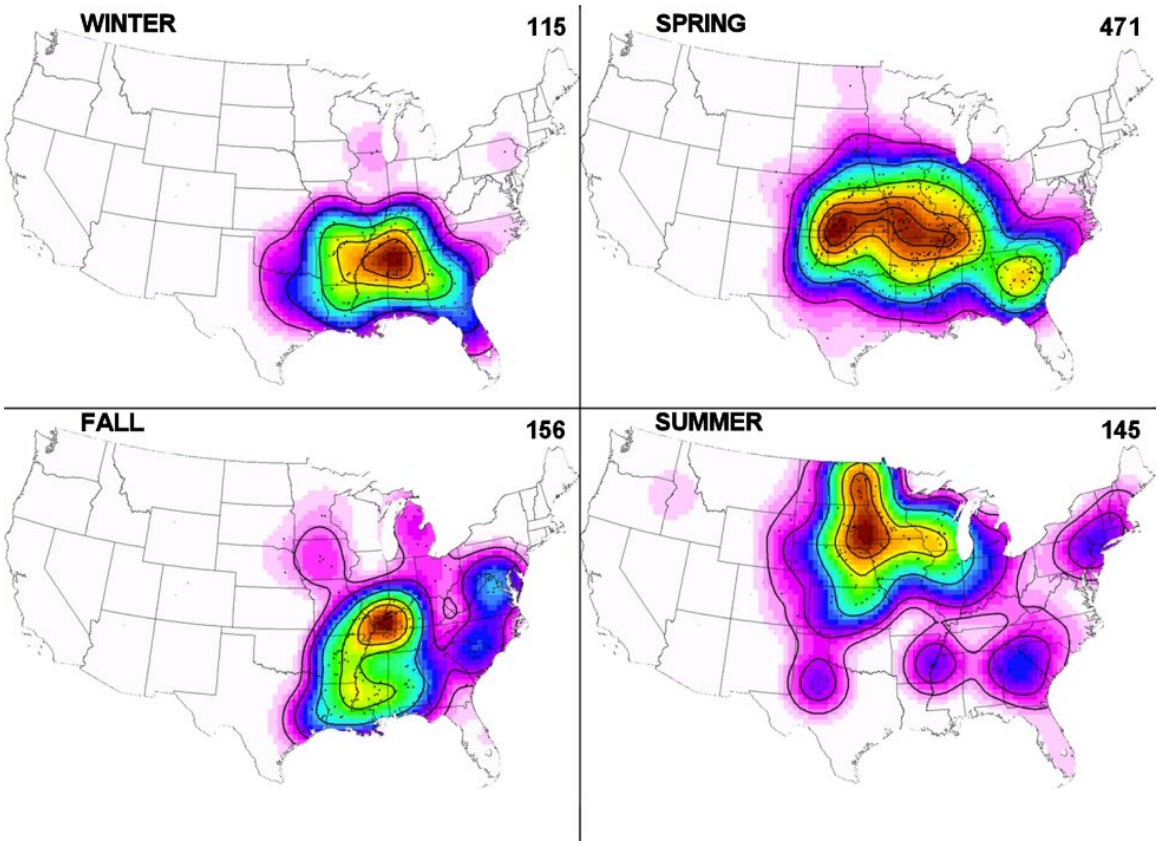

Figure 1. Seasonal kernel density estimation plots (based on the quadratic kernel function described in Silverman (1986, p. 76, equation 4.5)) of F2+ tornadoes produced by RM for winter (DEC-FEB), spring (MAR-MAY), summer (JUN-AUG), fall (SEP-NOV). The outermost black contour contains 90% of the kernel density estimation of events, with contours at 75%, 50%, 25% and 10%, with sample sizes in the upper right of each seasonal image (see S10 for additional information).

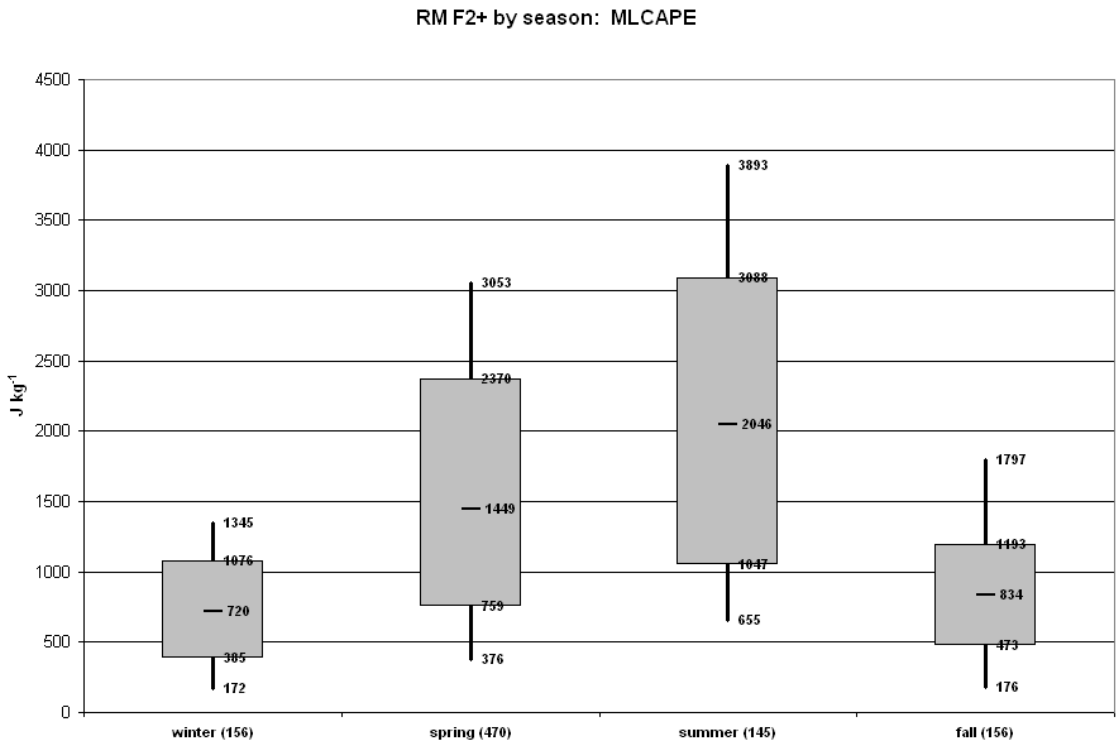

Figure 14. Seasonal box and whiskers plot of MLCAPE (J kg^{-1}) for RM that produced F2+ tornadoes. Plot conventions the same as Fig. 1.

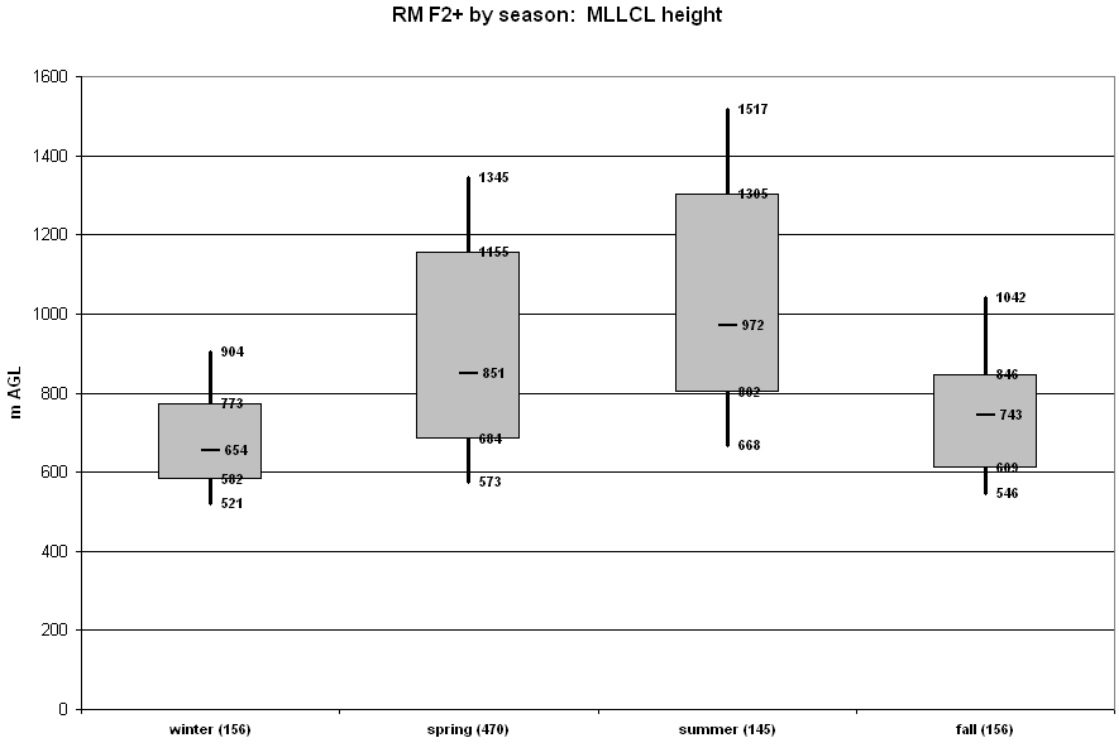

Figure 15. Same as Fig. 14, except for MLLCL height (m AGL).

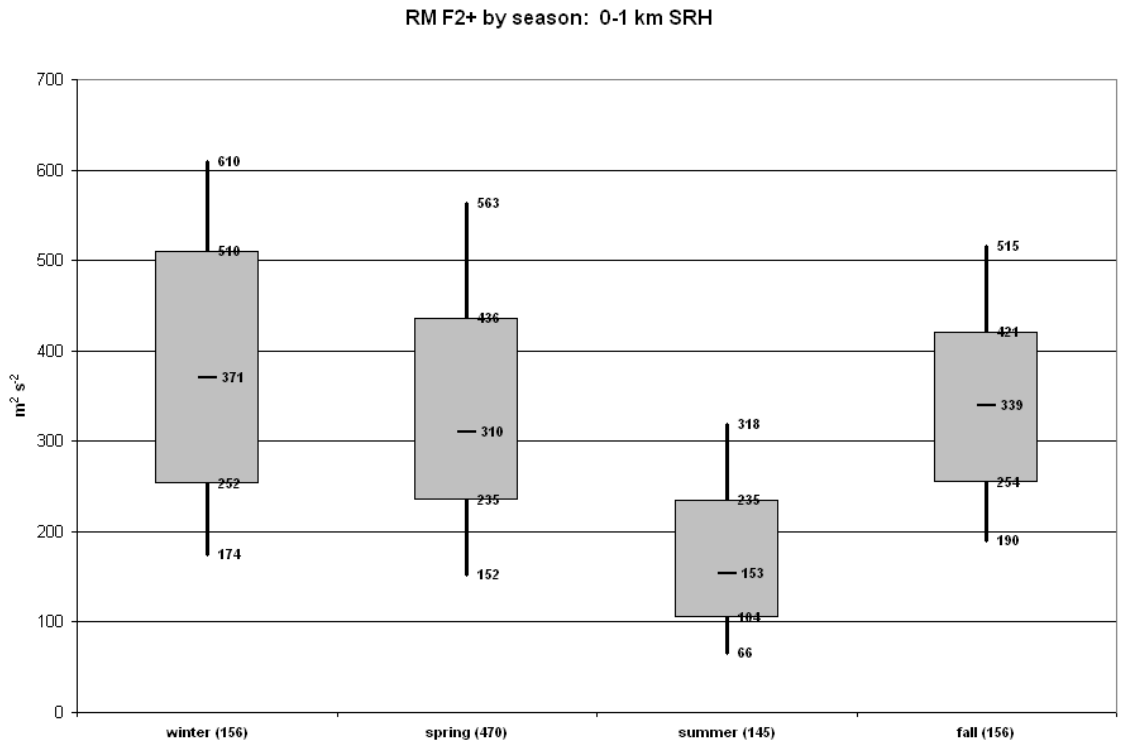

Figure 16. Same as Fig. 14, except for 0-1 km SRH ($m^2 s^{-2}$).

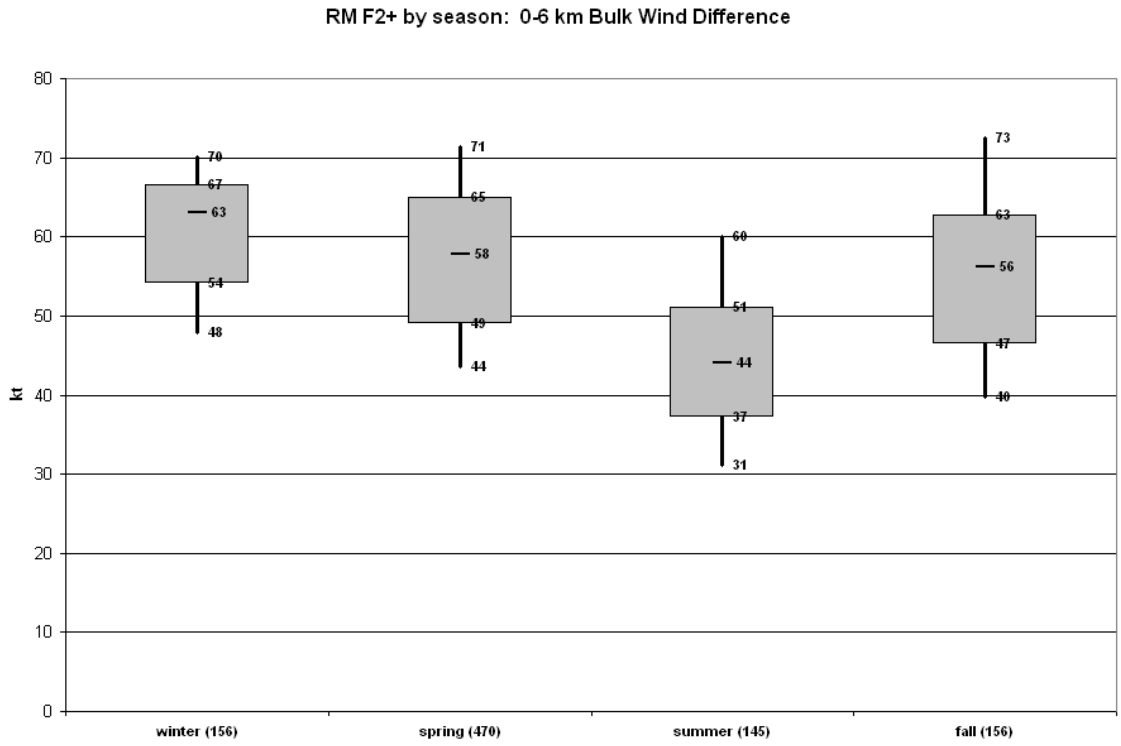

Figure 17. Same as Fig. 14, except for 0-6 km bulk wind difference (kt).

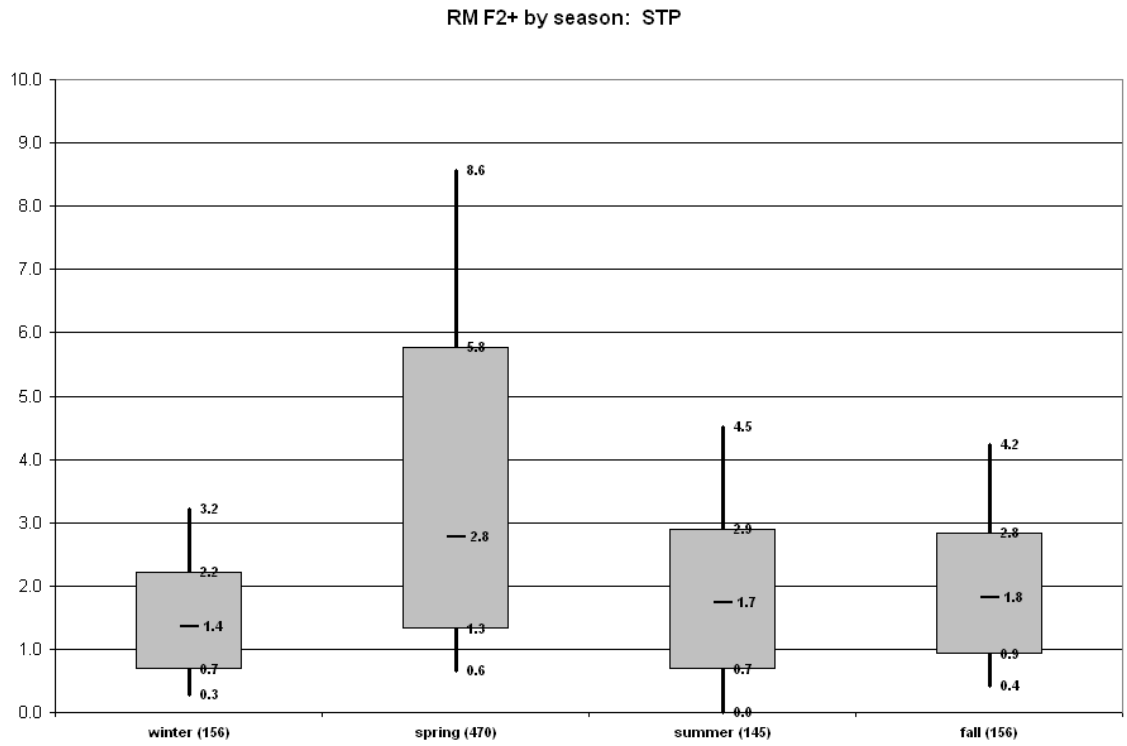

Figure 18. Same as Fig. 14, except for STP.